7-1-2006

Fluidized Bed Heat Treatment of Cast Al-Si-Cu-Mg Alloys

S. K. Chaudhury

Diran Apelian
Worcester Polytechnic Institute, dapelian@wpi.edu

Fluidized Bed Heat Treatment of Cast Al-Si-Cu-Mg Alloys

S.K. CHAUDHURY and D. APELIAN

The effects of fluidized bed heat treatment on the microstructural and mechanical properties of Al-Si-Cu-Mg cast alloys, namely, 354 and 319, were studied. The heating rate in fluidized beds (FBs) is greater *vis-à-vis* conventional electrical resistance furnaces (CFs). The high heating rate in FBs increases the kinetics of metallurgical phenomena such as Si fragmentation and spherodization during solution heat treatment, as well as the precipitation rate of phases such as $Al_5Cu_2Mg_8Si_6$ and Al_2Cu during aging. It is observed that the dissolution rate of phases such as Mg_2Si and $Al_5Cu_2Mg_8Si_6$ takes place very rapidly. The solution heat treatment of 319 alloy using FB results in complete dissolution of Mg_2Si and $Al_5Cu_2Mg_8Si_6$ particles within 45 minutes. However, for phases such as Al_2Cu and Fe-rich intermetallics, the dissolution rate is relatively slow. Even on prolonged solution heat treatment for 6 hours, these phases do not dissolve completely. It is observed that incomplete dissolution of the Al_2Cu phase does not significantly affect tensile properties of T4-treated alloys. The optimum solution heat-treatment time in FB for both 354 and 319 alloys is 45 minutes at 527 °C and 493 °C, respectively. Thermal analysis shows an exothermic peak owing to recrystallization and coarsening of eutectic grains during solution heat treatment. The high heating rate in FB causes this transformation to take place at a lower temperature than in CF. It is observed that the nucleation rate of $Al_5Cu_2Mg_8Si_6$ during aging in FB is greater than using CF. Thermal analysis of samples during the ramp-up stage while aging using FB did not show any phase transformation, while those using CF show two endothermic transformations, which are most likely due to the dissolution of GP zones or the co-cluster of solutes. Aging at 200 °C results in a greater number density of precipitates than those at 240 °C. The tensile strength of samples aged at 200 °C is greater than those aged at 240 °C, because the amount of precipitates formed at 200 °C is greater than that at 240 °C. The total heat-treatment time for T6 temper is less than 2 hours in FBs, which is a significant reduction in heat-treatment time, as well as energy consumption.

I. INTRODUCTION

THE strength of common hypoeutectic as-cast Al-Si-Cu-Mg alloys is in the range of 160 to 180 MPa.[1,2] Through heat treatment, the strength of these alloys can be increased by 80 to 90 pct of their as-cast strength.[3,4,5] Cast Al-Si-Cu-Mg (354 and 319) alloys are widely used in automotive, aerospace, transportation, and defense industries. In general, these alloys have reasonably good ductility, machinability, pressure tightness, and moderate strength properties.[3] The most common heat-treatment temper for these alloys is T6, which is comprised of solution heat treatment and quenching, followed by artificial aging. Solution heat treatment increases ultimate tensile strength (UTS) and ductility, while aging increases yield strength (YS) at the expense of ductility. Solution heat treatment results in the following microstructural changes: (1) dissolution of solutes, (2) spherodization of eutectic Si, (3) morphological changes of Fe- and Cu-rich intermetallics, (4) recrystallization of eutectic grains, and (5) homogenization. It may be noted that unlike in wrought alloys that are mechanically worked, the driving force for recrystallization in cast alloys is the thermal stress generated due to the thermal mismatch between Al and Si.

Solution heat treatment is carried out near the solidus temperature. In general, depending upon the Cu content, Al-Si-Cu-Mg alloys are solutionized between 480 °C and 525 °C, which is lower than the solutionizing temperature (~540 °C) for Al-Si-Mg alloys. This is because the solidus temperature often imposes a limitation to the maximum temperature at which solution heat treatment can be carried out. The Al-Si-Cu-Mg alloys contain the Al_2Cu phase that has a low melting point.[6,7] Hence, for Al-Si-Cu-Mg alloys, high solutionizing temperatures are not used to avoid incipient melting. As expected, with lower solutionizing temperatures, longer solutionizing times are required (~6 to 12 hours). In order to reduce the solutionizing time for 319 alloy, Sokolowski *et al.*[8] followed a two-step solution heat-treatment method, which involved a first step at 495 °C for 2 to 4 hours followed by a second step at 515 °C or 527 °C for 3 to 4 hours. The purpose of the first step, solution treatment at the lower temperature, is to dissolve the low melting point phase (Al_2Cu); whereas the second step, at a higher temperature, is intended to increase the homogenization kinetics and reduce the overall solution heat treating time. It is reported that the two-step solution heat treatment significantly improves casting properties (such as tensile strength, ductility, and impact toughness) *vis-à-vis* the one-step solution heat treatment at 495 °C.[8] After solution heat treatment, alloys are quenched to retain solutes and vacancy concentration at room temperature. It is important that components be quenched with minimum delay during their transfer from the furnace to the quench tank. The as-quenched alloys are either naturally aged at room temperature (commonly referred to as T4 temper) or artificially aged at a temperature between 150 °C and 240 °C.

S.K. CHAUDHURY, Research Associate, and D. APELIAN, Professor, are with the Metal Processing Institute (MPI), Worcester Polytechnic Institute (WPI), Worcester, MA 01609. Contact e-mail: sujoy@wpi.edu

Manuscript submitted August 19, 2005.

Aging causes precipitation of one or more of the phase(s) Mg_2Si, $Al_5Cu_2Mg_8Si_6$, or Al_2Cu in the Al-Si-Cu-Mg alloys depending upon the chemical composition.[9-12] These precipitates cause strengthening of the alloy.

Heat-treatment characteristics of Al-Si-Cu-Mg alloys have been investigated.[9,11] The precipitation strengthening response in these alloys is due to the decomposition of metastable supersaturated solid solution obtained by solution heat treatment and quenching. Phases that have been reported to precipitate during aging of Al-Si-Cu-Mg alloys (depending upon the chemical composition) are Al_2Cu (θ), Mg_2Si (β), $Al_5Cu_2Mg_8Si_6$, and Al_2CuMg (S) phases.[9-12] Kang *et al.*[12] reported that the θ' phase has a preferential tendency to precipitate on dislocations around Si particles, while the $Al_5Cu_2Mg_8Si_6$ phase homogeneously precipitates in the α-Al matrix. Zafar *et al.*[11] suggested that the $Al_5Cu_2Mg_8Si_6$ phase contributes significantly to the age-hardening behavior of these alloys, since it is uniformly distributed in the Al matrix. Li *et al.*[9] have reported that the precipitation sequence in Al-Si-Cu-Mg alloys is supersaturated solid solution → formation of Guinier-Preston (GP) zones → dissolution of GP zones → formation of metastable phase → formation of equilibrium phase. The aging sequence for these alloys is quite complicated and often two aging peaks are observed. The first peak of the age hardening curve is probably due to the high density of GP zones, while the formation of the metastable phase contributes to the second peak. Between the two peaks, the alloy has low strength.[9] This is because, at the intermediate stage of aging (*i.e.,* during the transition of GP zones to metastable phases), the density of GP zones is significantly low owing to their dissolution, while the semicoherent metastable precipitates are too small to offer any resistance to dislocation motion. Therefore, the age hardening curve shows a dip (low hardness) at this intermediate stage. Oullet *et al.*[13] studied the effect of Mg content and Sr modification on the heat treating characteristics of Al-Si-Cu-Mg alloys and observed that tensile strength improved significantly with Mg additions up to 0.45 wt pct, while the addition of Sr increased porosity and thereby reduced tensile strength. In addition, Sr-modified Al-Si-Cu-Mg alloys show severe segregation of Cu-rich intermetallics in areas away from the growing Si regions. However, Beumler *et al.*[14] observed that the addition of Mg in sand-cast Al-Si-Cu alloys has a negligible effect on tensile strength. In general, for Al-Si-Cu-Mg alloys, the duration of a T6 heat-treatment cycle using a conventional electrical furnace (CF) is about 12 to 20 hours.[4,5] Fluidized bed (FB) technology offers the advantage that the heat treat cycle can be shortened significantly, thus reducing costs and increasing manufacturing productivity.

A typical fluidized bed basically consists of a bed of finely divided particles, which are made to behave like a fluid by passing air through the orifice at the bottom of the furnace. A detailed description of modern FB furnaces can be found elsewhere.[15] The bed material in the FB used for this study is Staurolite sand ($Fe_2Al_9Si_4O_{22}(OH)_2$), and its particle size ranged from 80 to 120 μm. It has been reported that the heat-transfer coefficient is maximum for average particle size of about 100 μm.[16] The major benefit of the FB is that it has a high heating rate and better temperature control. The maximum temperature variation noted in our laboratory-type furnace was about 2 °C to 3 °C. Uniform heating of components is critical in order to obtain consistent mechanical properties. In a CF, the temperature may vary by 20 °C to 30 °C from one location to another within the furnace. The nonuniformity of the temperature within the furnace can severely affect component performance. In addition, the FB is environmentally friendly and does not require high maintenance costs. The focus of this study is to establish the microstructure-property relationship between the FB and CF heat-treated Al-Si-Cu-Mg alloys. Both 354 and 319 alloys were heat treated to T4 and T6 tempers using the FB and CF and their heat treating characteristics were studied.

II. EXPERIMENTAL METHODS

The 354 and 319 alloys were heat treated to T4 (solution heat treated, quenched, and naturally aged) and T6 tempers (solution heat treated, quenched, and artificially aged) using a FB furnace. The FB technology provides a high heating rate and excellent temperature control.[17] The high heating rate plays a significant role in microstructural evolution in these alloys such as dissolution of solutes (Cu- and Mg-rich intermetallics), spherodization of Si during solution heat treatment, and precipitation and coarsening rate during aging.[15,18] For comparative purposes, selective experiments were carried out using a CF.

The 354 alloy contains ~1.8 wt pct Cu, whereas 319 alloy has a high copper content (~3 to 4 wt pct); the 319 alloy used in this study contained 2.8 pct Cu and was cast by Montupet (Nogent Sur Oise, France) in the form of cylinder heads. The 354 alloy was procured from Amcast Industrial Corp. (Dayton, OH). The 354 alloy was cast in a permanent mold in the form of tensile bar with 2-in. gage length and 0.5-in. gage diameter, per ASTM specification B557. The chemical compositions of 354 and 319 alloys are given in Table I; these were measured using a standard spectrographic technique. Both 354 and 319 alloys were grain refined and modified with Sr.

A. *Heat Treatment*

Castings were heat treated to T4 and T6 tempers. Both 354 and 319 alloys were solutionized using the FB and CF at 527 °C and 493 °C, respectively, for various time intervals, as given in Table II. Times reported are isothermal holding times, *i.e.,* time at temperature, and do not include ramp-up time. Subsequent to solution heat treatment, castings were quenched in water at 25 °C. The incubation time between quenching and tensile testing for T4 tempered castings was 48 hours.

Both 354 and 319 alloys were aged at 200 °C and 240 °C for various time intervals using FB and CF. The heat-treatment schedule for aging (T6 temper) is shown in Table III.

Table I. Chemical Compositions of Alloys in Weight Percentage

Alloy	Si	Mg	Fe	Cu	Mn	Sr	Ti	Al
354	8.65	0.45	0.08	1.81	—	0.002	0.13	Balance
319	7.48	0.30	0.36	2.76	0.08	0.01	0.16	Balance

Table II. Solutionizing (T4) Schedule for 354 and 319 Alloys

Alloy	Solutionizing Temperature (°C)	Solutionizing Time (Minutes)					
		15	30	45	60	120	360
354	527	FB/CF	FB/CF	FB/CF	FB/CF	FB/CF	CF
319	493	FB	FB	FB	FB	FB	CF

Table III. Aging (T6) Schedule for 354 and 319 Alloys

Aging Temperature (°C)	Aging Time (Min)				
	30*	60*	120*	180*	300**
200	FB	FB	FB	FB	CF
240	FB	FB	FB	FB	CF

*Solutionized using FB for 45 min.
**Solutionized using CF for 360 min.

Prior to aging, both 354 and 319 alloys were solution heat treated at 527 °C and 493 °C, respectively, using the FB for 45 minutes and subsequently quenched in water at room temperature (25 °C). The incubation time between quenching and aging was 48 hours. In addition, some selected experiments on T6 temper (solutionized, water quenched, and aged) of 354 and 319 alloys were carried out using the CF. Alloys were aged using the CF at 200 °C and 240 °C for 300 minutes. Prior to aging in the CF, both 319 and 354 alloys were solutionized using a CF at 527 °C and 493 °C, respectively, for 360 minutes.

B. *Thermal Analysis*

Thermal analysis was carried out to study the phase transformation(s) during various stages of heat treatment. A phase transformation is accompanied by a release (exothermic) or absorption (endothermic) of thermal energy, which is usually detected by superimposing the first derivative curve (*i.e., dT/dt vs t*) on the heating profile (*i.e., T vs t*).[19] An exothermic event results in a sudden increase in *dT/dt* value, whereas an endothermic event results in a sudden decrease in *dT/dt* value at the starting point of the transformation. Temperature measurements were carried out using DASYLab software (National Instruments, Woburn, MA) coupled with a data acquisition system at an acquisition rate of 10 data points per second.

C. *Microstructural Characterization*

Microstructural analyses of both as-cast and heat-treated samples were carried out using optical microscopy and scanning electron microscopy (SEM). Samples for optical microscopy were prepared by the standard method of grinding and polishing using different grits of emery paper followed by polishing with alumina and silica gel. Samples for SEM were prepared by polishing with emery paper and electropolishing at 30 V for 20 seconds. The composition of the electrolyte (in volume percent) was 60 pct ethyl alcohol, 20 pct perchloric acid, and 20 pct ethylene glycol.

D. *Evaluation of Tensile Properties*

Mechanical properties (namely, UTS, YS, and elongation) of as-cast and heat-treated alloys were measured using an Instron tensile testing machine (model 5500R) and Merlin software (Instron, Norwood, MA) to control and record data. The 319 tensile specimens were machined from the cylinder heads; the gage cross section of tensile bars was 0.2 in. × 0.25 in. (rectangular cross section) with 1-in. gage length. The 354 tensile specimens were cast in the permanent mold; their dimensions were 0.5-in. gage diameter and 2-in. gage length. These dimensions are per ASTM standard specification. The tensile test was carried out at a 0.1-in./min extension rate, and an average of at least five test results were taken for each data point reported.

III. RESULTS AND DISCUSSION

Before presenting results on heat-treatment characteristics of Al-Si-Cu-Mg (354 and 319) alloys, it is important to discuss the effect of composition on the phase stability of these alloys as a function of temperature. Isopleths are vertical sections through ternary space diagrams and are quite useful in determining the heat-treatment schedule and its consequent effect on the resultant structure. Comparing vertical sections in multicomponent systems *vs* binary systems, the liquidus and solidus lines are not conjugate lines in multicomponent systems as they are in binary phase diagrams. Thus, isopleths are very useful in evaluating the role of composition and the safe operating window for heat treatment. Isopleth diagrams were simulated using PANDAT software, which calculates the most stable equilibrium phase using a global minimization algorithm based on mathematical and thermodynamic properties between the Gibbs energy function and the stable phase equilibrium.[20] PANDAT uses the CALPHAD method to calculate unknown multicomponent phase equilibrium information from known information available for lower-order systems.[21]

A. *Isopleths in Al-Si-Cu-Mg Alloys*

1. *354 alloy*

Isopleth diagrams were simulated to study the effect of Mg and Cu concentrations on the phase stability during the postsolidification heat treatment of 354 alloy. Figures 1(a) and (b) show isopleths of Al-9Si-0.2Fe-0.2Ti-0.4Mg-0.02Sr-(1.6-2)Cu and Al-9Si-1.8Cu-0.2Fe-0.2Ti-0.02Sr-(0.4-0.6)Mg alloy, respectively. In the former case, the concentration of Cu was varied from 1.6 to 2 wt pct with Mg concentration fixed at 0.4 wt pct (Figure 1(a)), and in the latter case, the concentration of Mg was varied from 0.4 to 0.6 wt pct with Cu concentration kept at 1.8 wt pct (Figure 1(b)).

Phases stable at different regions of the isopleth diagram (marked in Figure 1(a)), as a function of Cu content and temperature, are given as follows:

Region 1: $Si + Al_5Cu_2Mg_8Si_6 + Al_4Sr + Al_3Ti + Al_5FeSi + Al_2Cu + \alpha\text{-Al}$
Region 2: $Si + Al_5Cu_2Mg_8Si_6 + Al_4Sr + Al_3Ti + Al_5FeSi + \alpha\text{-Al}$
Region 3: $Si + Al_5Cu_2Mg_8Si_6 + Al_4Sr + \alpha\text{-Al} + Al_5FeSi + Al_2Cu$
Region 4: $Si + Al_5Cu_2Mg_8Si_6 + Al_4Sr + \alpha\text{-Al} + Al_5FeSi$
Region 5: $Si + Al_8FeMg_3Si_6 + Al_4Sr + \alpha\text{-Al} + Al_5FeSi$

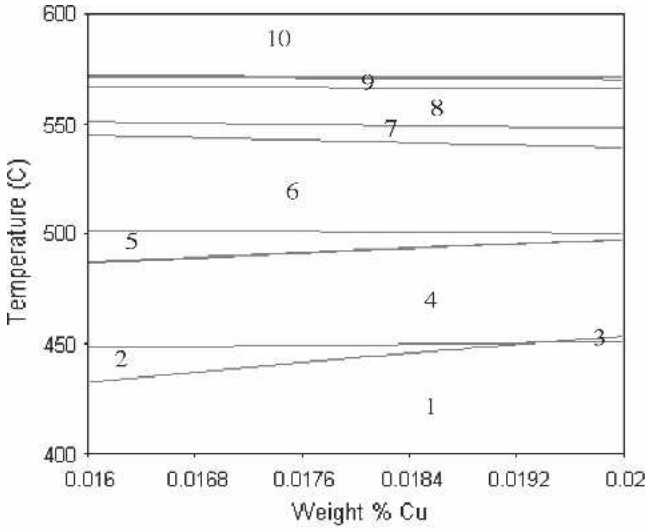

(*a*)

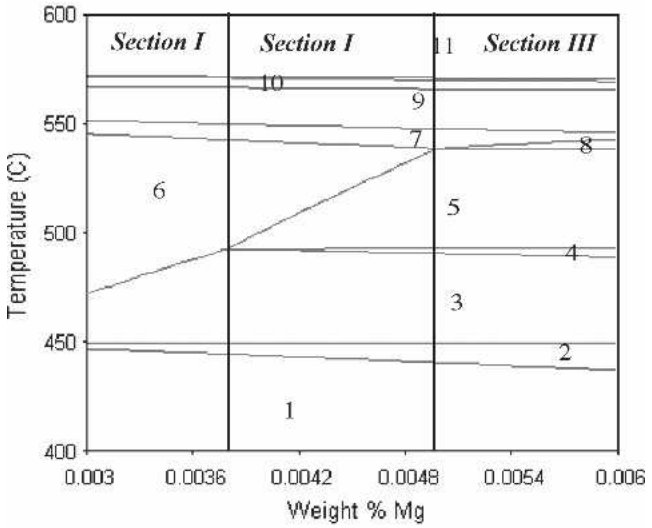

(*b*)

Fig. 1—(*a*) Isopleth diagram of Al-9Si-0.2Ti-0.2Fe-0.002Sr-0.4Mg-(1.6-2)Cu alloy (354) showing phases stable at different regions. These regions are (1) Si + $Al_5Cu_2Mg_8Si_6$ + Al_4Sr + Al_3Ti + Al_5FeSi + Al_2Cu + α-Al, (2) Si + $Al_5Cu_2Mg_8Si_6$ + Al_4Sr + Al_3Ti + Al_5FeSi + α-Al, (3) Si + $Al_5Cu_2Mg_8Si_6$ + Al_4Sr + α-Al + Al_5FeSi + Al_2Cu, (4) Si + $Al_5Cu_2Mg_8Si_6$ + Al_4Sr + Al_5FeSi + α-Al, (5) Si + $Al_8FeMg_3Si_6$ + Al_4Sr + Al_5FeSi + α-Al, (6) Si + Al_4Sr + Al_5FeSi + α-Al, (7) L + Al + Si + Al_4Sr + Al_5FeSi, (8) L + α-Al + Si + Al_5FeSi, (9) L + Al + Si, (10) L + Al_3Ti + Al. (*b*) Isopleth diagram of Al-9Si-0.2Ti-0.2Fe-0.002Sr-1.8Cu- (0.3 to 0.6) Mg alloy (354) showing phases stable at different regions. These regions are (1) Si + $Al_5Cu_2Mg_8Si_6$ + Al_4Sr + α-Al + Al_5FeSi + Al_2Cu, (2) Si + $Al_5Cu_2Mg_8Si_6$ + Al_4Sr + α-Al + Al_5FeSi + Al_3Ti, (3) Si + Al_4Sr + Al_5FeSi + α-Al + $Al_5Cu_2Mg_8Si_6$, (4) Si + $Al_5Cu_2Mg_8Si_6$ + Al_4Sr + α-Al + Al_5FeSi + $Al_8FeMg_3Si_6$, (5) Si + Al_4Sr + α-Al + Al_5FeSi + $Al_8FeMg_3Si_6$, (6) Si + Al_4Sr + α-Al + Al_5FeSi, (7) Si + Al_4Sr + Al_5FeSi + α-Al + L, (8) Si + Al_4Sr + Al_5FeSi + α-Al + $Al_8FeMg_3Si_6$ + L, (9) L + α-Al + Si +Al_5FeSi, (10) L + α-Al + Si, and (11) L + Al_3Ti + α-Al.

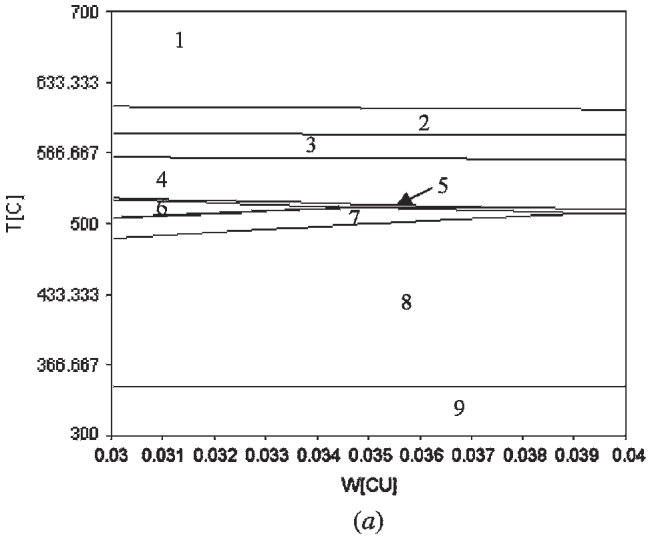

(*a*)

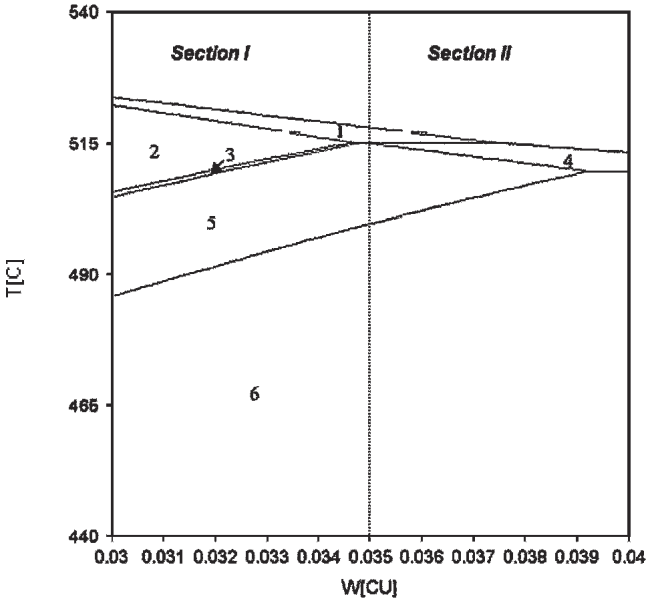

(*b*)

Fig. 2—(*a*) Isopleth diagram of Al-6Si-0.5Mg-0.5Fe alloy as a function of Cu concentration showing phases stable at different regions. These Regions are (1) L, (2) L + α-Al, (3) L + α-Al + Al_5FeSi, (4) L + Si + α-Al + Al_5FeSi, (5) L + Si + $Al_8FeMg_3Si_6$ α-Al + Al_5FeSi, (6) Si + $Al_8FeMg_3Si_6$ + α-Al + Al_5FeSi, (7) Si + $Al_5Cu_2Mg_8Si_6$ + α-Al + Al_5FeSi, (8) Si + $Al_5Cu_2Mg_8Si_6$ + α-Al + Al_5FeSi + Al_2Cu, (9) Si + Mg_2Si + α-Al + Al_5FeSi + Al_2Cu. (*b*) Isopleth diagram of Al-6Si-0.5Fe-0.5Mg alloy as a function of Cu concentrations in the temperature range between 440 °C to 540 °C showing phases stable at different regions. These regions are (1) L + Si + $Al_8FeMg_3Si_6$ + α-Al + Al_5FeSi, (2) Si + $Al_8FeMg_3Si_6$ + α-Al + Al_5FeSi, (3) Si + $Al_5Cu_2Mg_8Si_6$ + α-Al + Al_5FeSi + $Al_8FeMg_3Si_6$, (4) Si + $Al_5Cu_2Mg_8Si_6$ + α-Al + Al_5FeSi + L, (5) Si + $Al_5Cu_2Mg_8Si_6$ + α-Al + Al_5FeSi, and (6) Si + $Al_5Cu_2Mg_8Si_6$ + α-Al + Al_5FeSi + Al_2Cu.

Region 6: Si + Al_4Sr + α-Al + Al_5FeSi
Region 7: L + α-Al + Si + Al_4Sr + Al_5FeSi
Region 8: L + α-Al + Si + Al_5FeSi
Region 9: L + α-Al + Si
Region 10: L + Al_3Ti + α-Al

At the solutionizing temperature of 527 °C, the isopleth diagram predicts complete dissolution of solute atoms such as Cu and Mg in the Al matrix. The amount of Mg content in the supersaturated Al matrix (after quenching from solution heat-treatment temperature) is critical and has a significant effect on the mechanical properties of the alloy.

The effect of Mg content on phase stability is shown in Figure 1(b). Phases stable at different regions of the isopleth (marked in the Figure 1(b)) are given subsequently:

Region 1: Si + $Al_5Cu_2Mg_8Si_6$ + Al_4Sr + α-Al + Al_5FeSi + Al_2Cu
Region 2: Si + $Al_5Cu_2Mg_8Si_6$ + Al_4Sr + α-Al + Al_5FeSi + Al_3Ti
Region 3: Si + $Al_5Cu_2Mg_8Si_6$ + Al_4Sr + α-Al + Al_5FeSi
Region 4: Si + $Al_5Cu_2Mg_8Si_6$ + Al_4Sr + α-Al + Al_5FeSi + $Al_8FeMg_3Si_6$
Region 5: Si + Al_4Sr + α-Al + Al_5FeSi + $Al_8FeMg_3Si_6$
Region 6: Si + Al_4Sr + α-Al + Al_5FeSi
Region 7: Si + Al_4Sr + α-Al + Al_5FeSi + L
Region 7: Si + Al_4Sr + α-Al + Al_5FeSi + $Al_8FeMg_3Si_6$ + L
Region 8: L + α-Al + Si + Al_5FeSi
Region 9: L + α-Al + Si
Region 10: L + Al_3Ti + α-Al

The isopleth can be divided into three sections as a function of Mg content (Figure 1(b)):

Section I with Mg concentration less than 0.38 wt pct
Section II with Mg concentration greater than 0.38 wt pct and less than 0.49 wt pct
Section III with Mg concentration greater than 0.49 wt pct and less than 0.6 wt pct

In Section I, phases stable at solution heat treating temperatures between 515 °C and 527 °C are Si + Al_4Sr + α-Al + Al_5FeSi. This shows that both Mg and Cu are in solid solution of the Al matrix per the equilibrium isopleth diagram. In contrast, when the Mg concentration is greater than 0.38 pct and less than 0.49 pct (Section II), phases stable at solution heat treating temperatures between 515 °C and 527 °C can be either (Si + Al_4Sr + α-Al + Al_5FeSi + $Al_8FeMg_3Si_6$) or (Si + Al_4Sr + α-Al + Al_5FeSi), depending on the Mg composition and temperature of solution heat treatment. In other words, the solution heat treatment of 354 alloy with Mg concentration in Section II will result in either complete or partial transformation of Al_5FeSi phase to $Al_8FeMg_3Si_6$ phase, since the $Al_8FeMg_3Si_6$ phase is likely to be retained during postsolution heat treatment. In Section III, with Mg concentration greater than 0.49 pct, phases stable are Si + Al_4Sr + α-Al + Al_5FeSi + $Al_8FeMg_3Si_6$. Hence, with Mg concentration greater than 0.49 pct, the volume fraction of $Al_8FeMg_3Si_6$ phase will be greater than the Al_5FeSi phase. This shows incomplete dissolution of Mg in the Al matrix, since $Al_8FeMg_3Si_6$ will most likely be retained after solution heat treatment. The amount of solute retained in the matrix will play a vital role in the postaging treatment of the alloy. Further, it may be noted that the Al_5FeSi is the equilibrium phase in the as-cast condition. The Al_5FeSi phase has a typical faceted morphology with sharp angular edges,[22,23] which act as stress concentrators and may have deleterious effects on mechanical properties. In contrast, the $Al_8FeMg_3Si_6$ phase has a typical Chinese script–like morphology with curved edges,[24] which are relatively less harmful than the Al_5FeSi phase. It is quite evident that the alloy composition is quite critical and plays an important role on the evolution of phases and microstructure during postsolidification heat treatment.

2. *319 alloy*

Isopleth diagrams for the 319 alloy were obtained by varying Cu (3 to 4 pct) and Mg (0 to 1 pct) contents separately while keeping other elements fixed. In case 1, Cu was varied from 3 to 4 pct, keeping concentrations of Si, Fe, and Mg at 7, 0.5, and 0.5 pct, respectively. In case 2, Mg was varied from 0 to 1 pct while maintaining the concentrations of Si, Fe, and Cu at 7, 0.5, and 3.5 pct, respectively. The influence of Cu concentration on the equilibrium phase diagram is shown in Figure 2(a).

The sequence of phase transformations during solidification of the 319 alloy is given as follows (Figure 2(a)):

Region 1: Liquid
Region 2: Liquid + α-Al
Region 3: Liquid + α-Al + Al_5FeSi
Region 4: Liquid + Si + α-Al + Al_5FeSi
Region 5: Liquid + Si + $Al_8FeMg_3Si_6$ + α-Al + Al_5FeSi
Region 6: Si + $Al_8FeMg_3Si_6$ + α-Al + Al_5FeSi
Region 7: Si + $Al_5Cu_2Mg_8Si_6$ + α-Al + Al_5FeSi
Region 8: Si + $Al_5Cu_2Mg_8Si_6$ + α-Al + Al_5FeSi + Al_2Cu
Region 9: Si + Mg_2Si + α-Al + Al_5FeSi + Al_2Cu

It is interesting to note that the phase transformation continues even after solidification is completed, *i.e.,* in the solid state. To understand the role of the Cu concentration on microstructural evolution during solution heat treatment, the isopleth was simulated between 540 °C and 440 °C

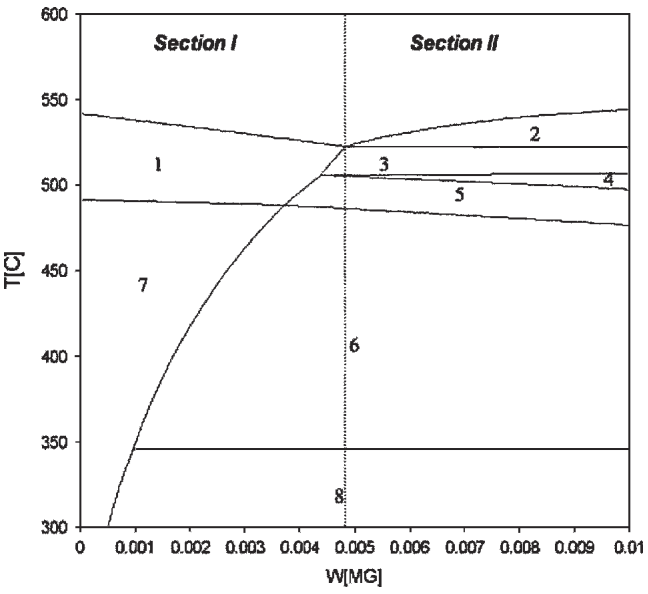

Fig. 3—Isopleth diagram of Al-6Si-3Cu-0.5Fe as a function of Mg concentrations showing phases stable at different regions. These regions are (1) Si + α-Al + Al_5FeSi, (2) L + Si + $Al_8FeMg_3Si_6$ + α-Al + Al_5FeSi, (3) Si + $Al_8FeMg_3Si_6$ + α-Al + Al_5FeSi, (4) Si + $Al_5Cu_2Mg_8Si_6$ + α-Al + Al_5FeSi + $Al_8FeMg_3Si_6$, (5) Si + $Al_5Cu_2Mg_8Si_6$ + α-Al + Al_5FeSi, (6) Si + $Al_5Cu_2Mg_8Si_6$ + α-Al + Al_5FeSi + Al_2Cu, (7) Si + α-Al + Al_5FeSi + Al_2Cu, and (8) Si + α-Al + Al_5FeSi + Al_2Cu + Mg_2Si.

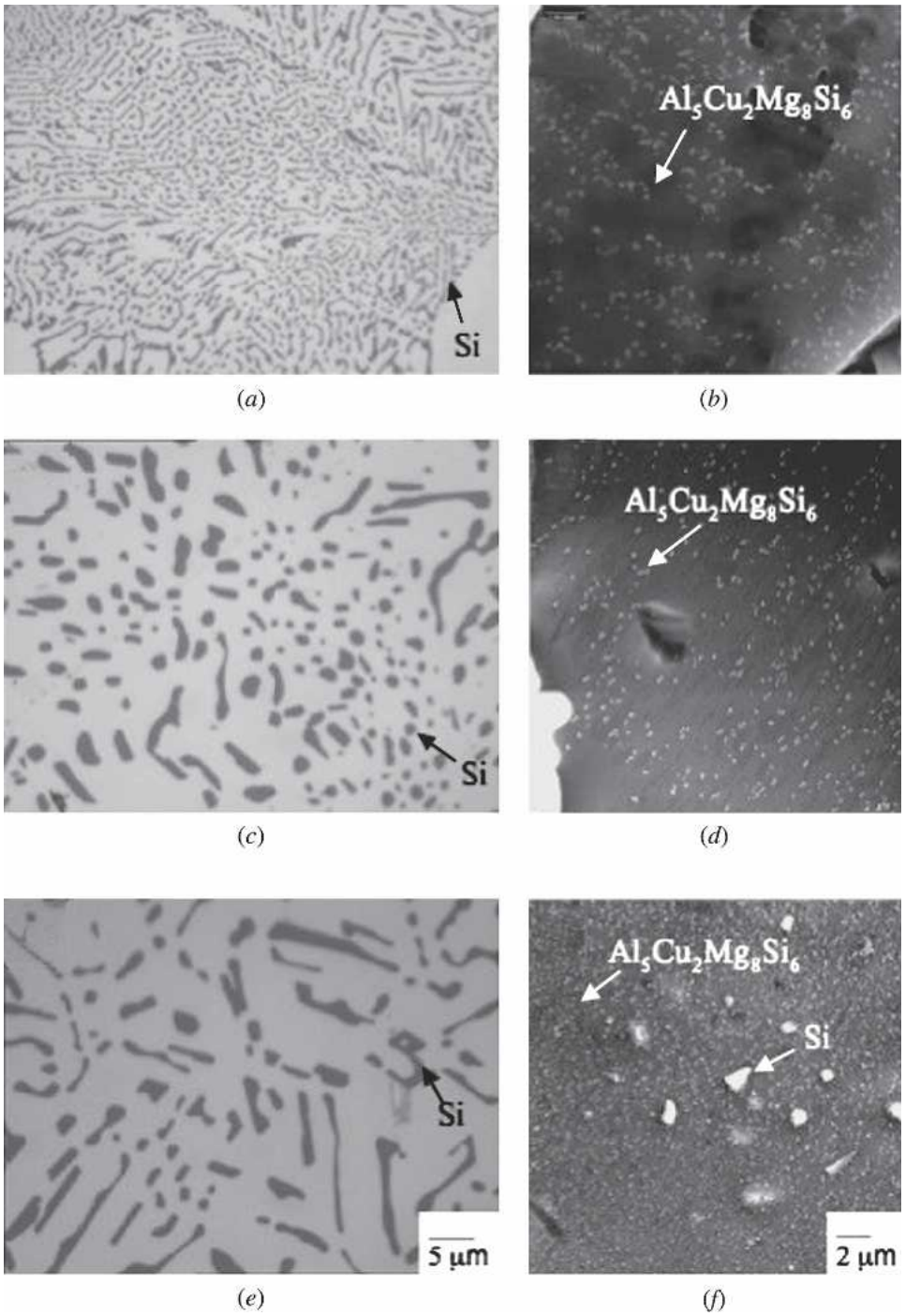

Fig. 4—Micrograph of 354 alloy in as-cast state. (*a*) Optical micrograph (eutectic region) and (*b*) SEM micrograph (dendritic region), solutionized using an FB reactor at 527 °C at 30 min. (*c*) Optical micrograph (eutectic region) and (*d*) SEM micrograph (dendritic region), solutionized using CF at 527 °C for 30 min. (*e*) Optical micrograph (eutectic region) and (*f*) SEM micrograph (dendritic region).

(Figure 2(b)). The sequence of regions is shown below for two different sections: Cu from 3 to 3.5 pct (section I) and Cu content higher than 3.5 pct (section II) (Figure 2(b)):

Region 1: Liquid + Si + $Al_8FeMg_3Si_6$ + α-Al + Al_5FeSi
Region 2: Si + $Al_8FeMg_3Si_6$ + α-Al + Al_5FeSi
Region 3: Si + $Al_5Cu_2Mg_8Si_6$ + α-Al + Al_5FeSi + $Al_8FeMg_3Si_6$
Region 4: Si + $Al_5Cu_2Mg_8Si_6$ + α-Al + Al_5FeSi + Liquid
Region 5: Si + $Al_5Cu_2Mg_8Si_6$ + α-Al + Al_5FeSi
Region 6: Si + $Al_5Cu_2Mg_8Si_6$ + α-Al + Al_5FeSi + Al_2Cu

When the concentration of Cu is greater than 3.5 pct (section II), there is a risk of incipient melting during solution heat treatment in the temperature range of 505 °C to

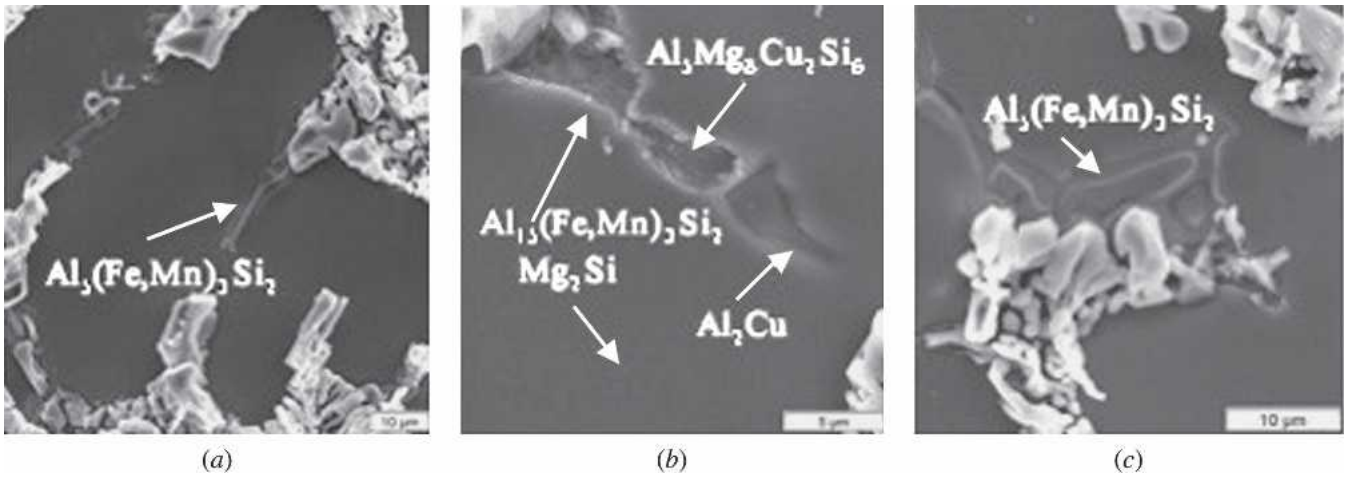

Fig. 5—SEM micrograph of as-cast 319 alloy: (*a*) eutectic Si; (*b*) intermetallics such as Mg_2Si, Al_2Cu, $Al_{15}(Fe,Mn)_3Si_2$, and $Al_5Mg_8Cu_2Si_6$; and (*c*) Fe-rich phase.

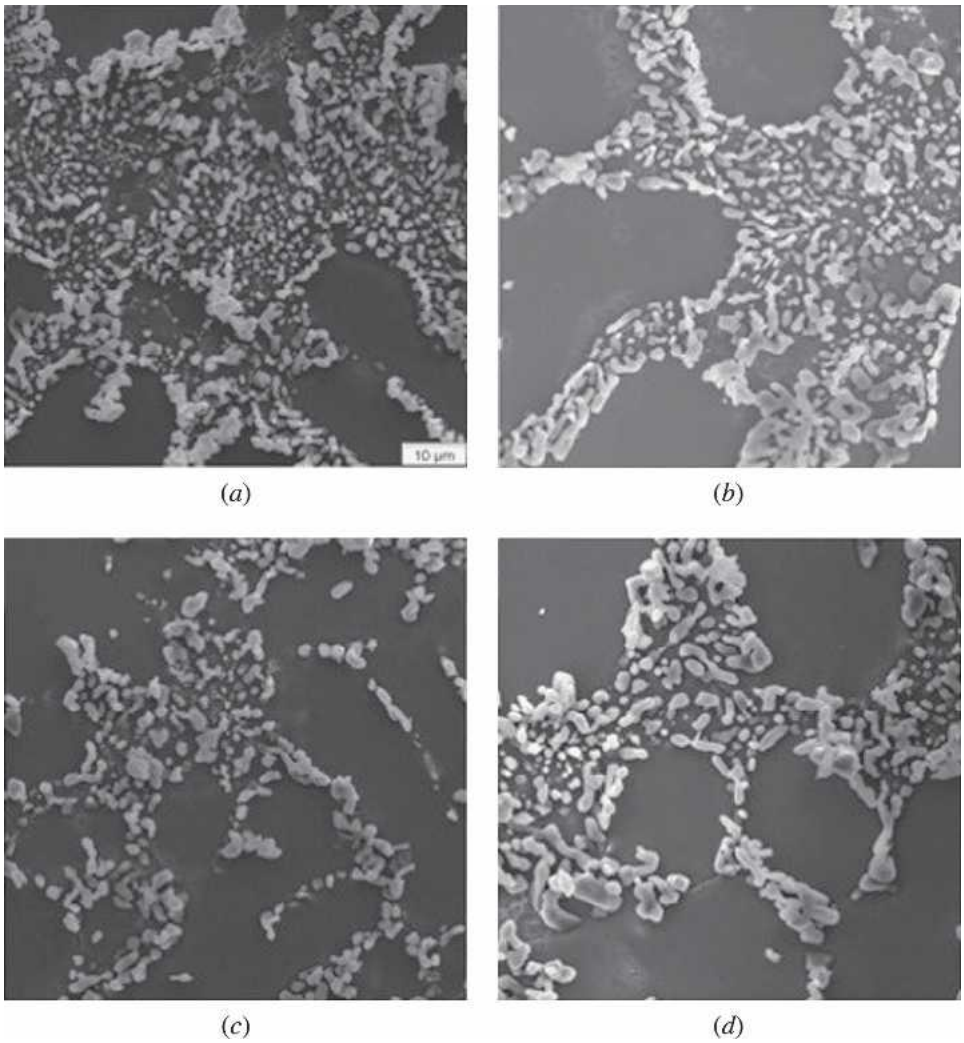

Fig. 6—Effect of the solution heat treatment on the morphology of eutectic Si of 319 alloy using an FB reactor at 493 °C for (*a*) 15 min, (*b*) 30 min, (*c*) 60 min, and (*d*) 120 min.

515 °C, as shown by region 4. In contrast, there is no risk of incipient melting during solution heat treatment at 515 °C, when the Cu concentration is less than 3.5 pct since only solid-state reactions take place (shown by regions 2 and 3). Accordingly, phases formed in the as-quenched state will either consist of Si, $Al_8FeMg_3Si_6$, α-A1, and Al_5FeSi (region 2) or Si, $Al_5Cu_2Mg_8Si_6$, α-Al, Al_5FeSi, and $Al_8FeMg_3Si_6$ (region 3) particles. The former (region 2)

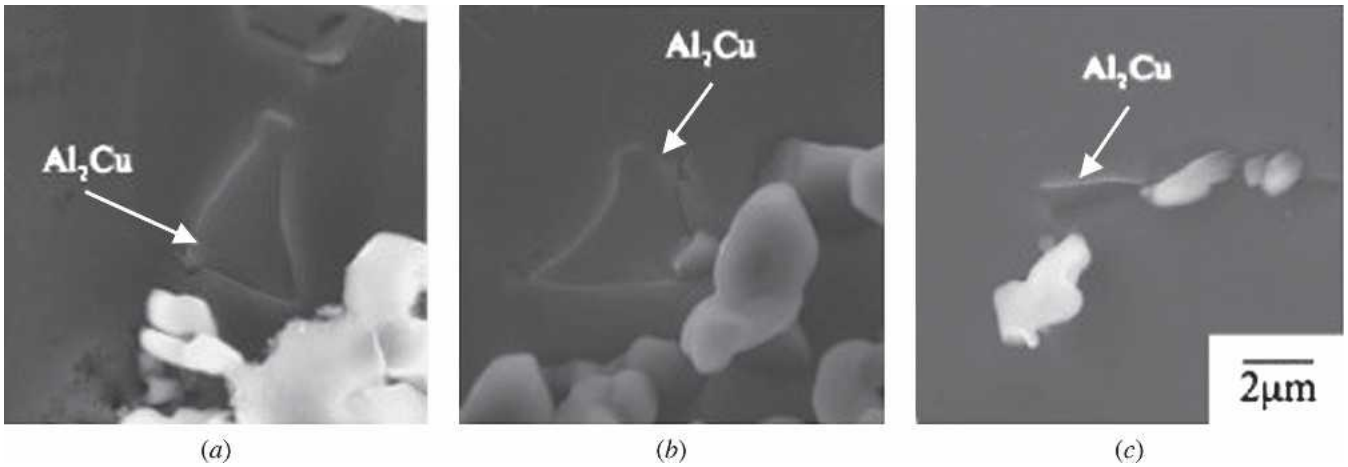

Fig. 7—Effect of the solution heat treatment of 319 alloy using an FB reactor at 493 °C on the morphology of Al_2Cu particles for (*a*) 30 min, (*b*) 60 min, and (*c*) 120 min.

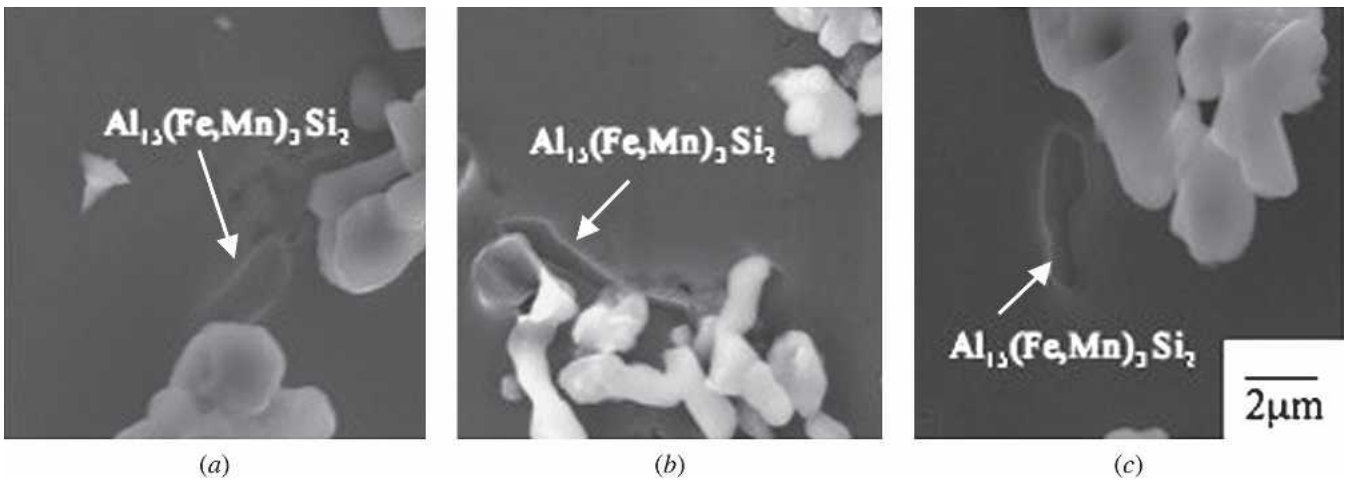

Fig. 8—Effect of the solution heat treatment of 319 alloy using an FB reactor at 493 °C on the morphology of $Al_{15}(Fe,Mn)_3Si_2$ particles for (*a*) 30 min, (*b*) 60 min, and (*c*) 120 min.

will lead to the complete dissolution of Cu in the Al matrix, while in the latter case (region 3), the $Al_5Cu_2Mg_8Si_6$ particles will be retained in the as-quenched state. Thus, the concentration of Cu plays a vital role in deciding the phase transformation event(s) and, hence, the microstructural evolution during postsolidification heat-treatment stage(s).

To understand the effect of Mg concentration (case 2) on microstructural evolution during solution heat treatment of 319 alloy, concentrations of Mg were varied from 0 to 1 pct, keeping concentrations of Cu, Si, and Fe at 3, 6, and 0.5 pct, respectively (Figure 3). Various phase transformation reactions (obtained by varying Mg concentration) in 319 alloy are shown as follows (Figure 3):

Region 1: $Si + \alpha\text{-}Al + Al_5FeSi$
Region 2: $Liquid + Si + Al_8FeMg_3Si_6 + \alpha\text{-}Al + Al_5FeSi$
Region 3: $Si + Al_8FeMg_3Si_6 + \alpha\text{-}Al + Al_5FeSi$
Region 4: $Si + Al_5Cu_2Mg_8Si_6 + \alpha\text{-}Al + Al_5FeSi + Al_8FeMg_3Si_6$
Region 5: $Si + Al_5Cu_2Mg_8Si_6 + \alpha\text{-}Al + Al_5FeSi$
Region 6: $Si + Al_5Cu_2Mg_8Si_6 + \alpha\text{-}Al + Al_5FeSi + Al_2Cu$
Region 7: $Si + \alpha\text{-}Al + Al_5FeSi + Al_2Cu$
Region 8: $Si + \alpha\text{-}Al + Al_5FeSi + Al_2Cu + Mg_2Si$

The isopleth diagram (Figure 3) is divided into two distinct sections: section I with Mg concentrations less than 0.48 pct and section II with Mg concentrations greater than 0.48 pct. In the case of Mg concentrations below 0.48 pct, phases stable at solution heat-treating temperatures between 505 °C and 515 °C are α-Al, Si, and Al_5FeSi. This shows that both Mg and Cu are in solid solution. In contrast, when Mg concentration is greater than 0.48 pct, phases stable at solution heat-treating temperatures between 505 °C and 515 °C can be products shown in either region 3 or 4, depending upon the concentration and the solution heat-treating temperature. Thus, solution heat treating the 319 alloy, with the Mg concentration greater than 0.48 pct, will result in partial dissolution of Mg and Cu as phases such as $Al_8FeMg_3Si_6$ and $Al_5Cu_2Mg_8Si_6$ are likely to be retained on quenching from the solutionizing temperature.

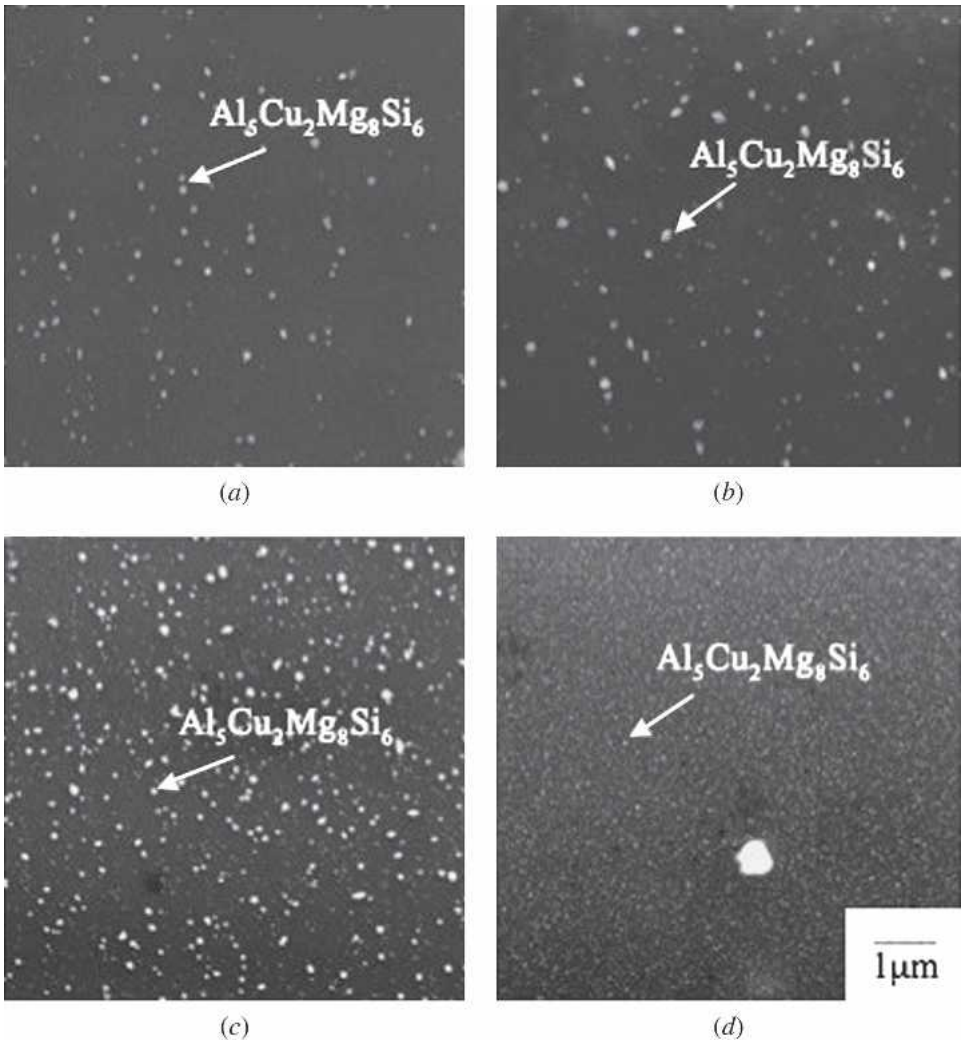

Fig. 9—SEM micrograph of 354 alloy solutionized in the FB at 527 °C for 45 min, quenched in water, and aged using the FB at 200 °C for (*a*) 30 min, (*b*) 60 min, and (*c*) 120 min and (*d*) aged using a CF for 300 min at 200 °C.

B. *Microstructural Observations*

1. *Solution heat treatment*

a. *354 alloy*

The effect of solution heat treatment on the microstructure of 354 alloy at 527 °C for 30 minutes using the FB and CF is shown in Figures 4(c) through (f), respectively. The as-cast structure (Figures 4(a) and (b)) typically consists of α-Al dendrites, eutectic Si, Fe-, and Cu-rich intermetallics. The energy dispersive X-ray (EDX) analyses reveal that these intermetallics are $Al_8FeMg_3Si_6$, $Al_5Cu_2Mg_8Si_6$, and Al_2Cu particles. The iron-rich intermetallics are distributed in the eutectic region as Chinese script and have angular edges. The $Al_5Cu_2Mg_8Si_6$ phase has a spherical morphology and is nonuniformly distributed in the Al matrix in the form of agglomerates. These are segregated along the edge of dendrites in the as-cast condition (Figure 4(b)). The solution heat treatment of 354 alloy for 30 minutes results in a noticeable reduction of macrosegregation of $Al_5Cu_2Mg_8Si_6$ particles (as shown in Figure 4(d)). On the other hand, dissolution kinetics of $Al_5Cu_2Mg_8Si_6$ particles in Al matrix during solution heat treatment using CF is relatively slow (Figure 4(f)). Two hours were needed *via* the CF for the $Al_5Cu_2Mg_8Si_6$ phase to dissolve in the Al matrix. The dissolution rate of solute phase ($Al_5Cu_2Mg_8Si_6$) in the Al matrix is higher when treated in the FB *vis-à-vis* CF. This is due to the morphological changes of solute phase ($Al_5Cu_2Mg_8Si_6$) during the initial heating stage prior to isothermal holding. The low heating rate in CF decreased the matrix/solute interfacial area due to coarsening of the agglomerate ($Al_5Cu_2Mg_8Si_6$ particles) during the ramp-up stage and thereby decreases the driving force for dissolution of solute phase.

In contrast, due to the high heating rate in the FB, solute agglomerates do not have sufficient time to coarsen and consequently dissolution begins to take place. Similarly, Caudillo *et al.*[25] observed that the dissolution rate of carbides in a CoCr-Mo-C alloy decreased with the decrease in the heating rate. This effect has been attributed to the morphological changes induced in the interdendritic precipitates during the heating stage. A slower heating rate decreases the matrix/precipitate interfacial area due to coarsening of carbide agglomerates and hence reduces the driving force for dissolution of the solute phase. The alloy

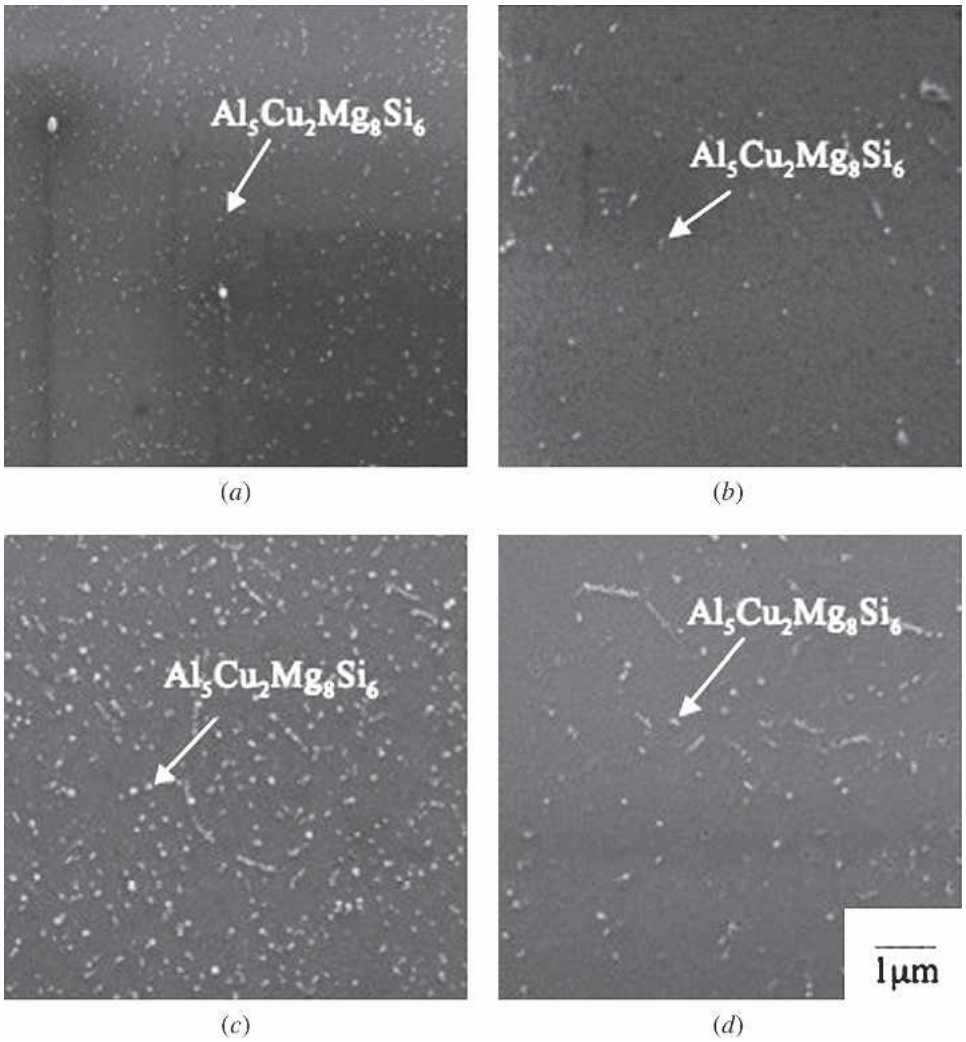

Fig. 10—SEM micrograph of 354 alloy solutionized in the FB at 527 °C for 45 min, quenched in water, and aged using the FB at 240 °C for (*a*) 30 min, (*b*) 60 min, and (*c*) 120 min and (*d*) aged using a CF for 300 min at 240 °C.

contains Al_2Cu phase (as another Cu-rich phase) in addition to $Al_5Cu_2Mg_8Si_6$ phase. The morphology of Al_2Cu phase is blocky type, which remains unaffected after solution heat treatment using both the FB and CF. The slow dissolution rate of Al_2Cu phases during solution heat treatment is attributed to their lower interfacial area (large blocky morphology) and slower interface mobility due to curvature effects (faceted morphology)[26] that consequently lower the driving force for dissolution of the Al_2Cu phase in the Al matrix.

The effect of solution heat treatment on the morphology of Si using the FB and CF is shown in Figures 4(c) and (e), respectively. It is observed that the breakdown of Si structure takes place within 15 to 30 minutes in both the FB and CF; however, during FB processing, a significant degree of spherodization is achieved within 45 to 60 minutes, while it took 120 minutes to achieve the same using the CF.

b. *319 alloy*

The as-cast microstructure (Figures 5(a) through (c)) of Sr-modified 319 alloy consists of the primary α-Al phase forming a dendritic network, and interdendritic eutectic phases consisting of eutectic Si and some intermetallic particles. Silicon particles exhibit a fibrous morphology having a coral-like structure; similar observations have been made elsewhere.[4,5] In addition to the eutectic Si phase, the as-cast microstructure also consists of the following intermetallics: (a) blocky Al_2Cu (θ) particles (Figure 5(b)), (b) spherical $Al_5Cu_2Mg_8Si_6$ particles (Figure 5(b)), (c) globular (Figure 5(b)) or Chinese script (Figure 5(c)) type $Al_{15}(Fe,Mn)_3Si_2$ particles, and (e) nonuniformly distributed needle-shaped Mg_2Si particles (Figure 5(b)). The spherical $Al_5Cu_2Mg_8Si_6$ particles are observed to nucleate on $Al_{15}(Fe,Mn)_3Si_2$ particles (Figure 5(b)). The Mg_2Si particles are mostly seen at the center of the dendrite.

Figures 6(a) through (d) show the effect of solution heat treatment on the morphology of eutectic Si at 493 °C for 15, 30, 60, and 120 minutes, respectively, using the FB. Microstructures reveal that the breakdown of eutectic Si takes place within the first 15 minutes using the FB. Beyond 60 minutes of solution heat treatment, the change in sphericity was marginal. The coarsening of eutectic Si takes place *via* Ostwald ripening, where large particles grow at the expense of small particles. In addition to

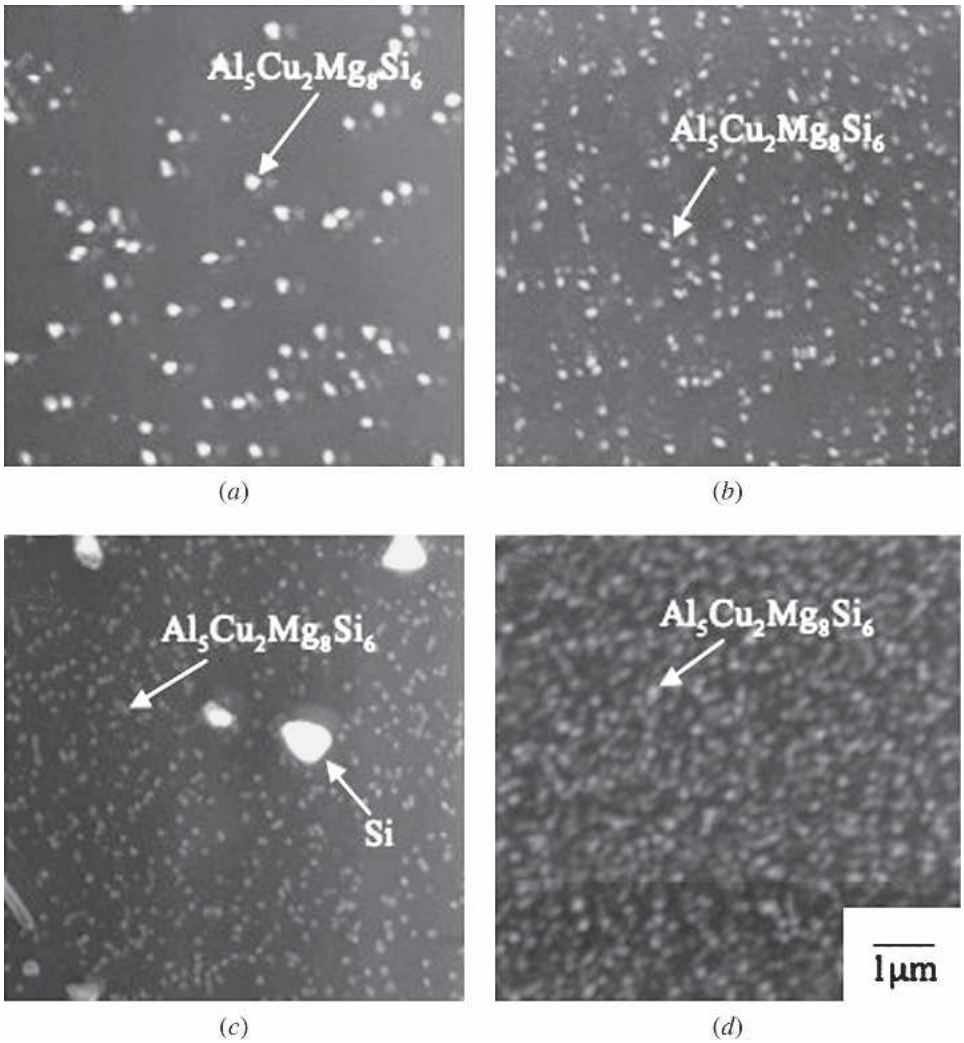

Fig. 11—SEM micrograph of 319 alloy solutionized in the FB at 493 °C for 45 min, quenched in water, and aged using the FB at 200 °C for (*a*) 30 min, (*b*) 60 min, and (*c*) 120 min and (*d*) aged using a CF for 300 min at 200 °C.

structural changes of eutectic Si particles, solution heat treatment of 319 alloy results in morphological changes of intermetallics such as Al_2Cu, $Al_{15}(Fe,Mn)_3Si_2$, Mg_2Si, and $Al_5Cu_2Mg_8Si_6$. Effects of solution heat treatment on intermetallics, namely, Al_2Cu and $Al_{15}(Fe,Mn)_3Si_2$, using FB are shown in Figures 7(a) through (c) and 8(a) through (c), respectively, for various solution heat-treatment times. Solution heat treatment using the FB results in the complete dissolution of Mg_2Si and $Al_5Cu_2Mg_8Si_6$ intermetallic particles within 30 minutes. In addition, the other intermetallics such as Al_2Cu and $Al_{15}(Fe,Mn)_3Si_2$ undergo partial dissolution. The complete dissolution of Al_2Cu and $Al_{15}(Fe,Mn)_3Si_2$ phases is not observed on solution heat treating even for 2 hours using the FB. The reduction in size of the Al_2Cu phase takes place through dissolution, while that of $Al_{15}(Fe,Mn)_3Si_2$ phase takes place through fragmentation.

2. *Aging*

a. *354 alloy*

The microstructure of FB-aged components at 200 °C and 240 °C (for 60 minutes) containing precipitates of $Al_5Cu_2Mg_8Si_6$ and Mg_2Si particles are shown in Figures 9 and 10, respectively. These phases were identified through EDX analysis. Microstructures reveal uniformly distributed spherical $Al_5Cu_2Mg_8Si_6$ particles in the Al matrix. The uniform distribution of these particles in the Al matrix is evidence that, through solution heat treatment at 527 °C for 45 minutes, the microsegregation of Si, Cu, and Mg were significantly reduced. The dominant mechanism of coarsening of $Al_5Cu_2Mg_8Si_6$ particles is through coalescence of smaller particles. It is interesting to note that, during the initial stages of nucleation of $Al_5Mg_8Cu_2Si_6$ particles, the particles form clusters,[9] which subsequently join together and coarsen. In general, the precipitation rate is higher when aged at 200 °C as compared to 240 °C. Precipitation and coarsening rates of $Al_5Cu_2Mg_8Si_6$ are greater in the FB-aged alloys *vis-à-vis* CF aged.

b. *319 alloy*

The microstructures of FB-aged components at 200 °C and 240 °C for different times are shown in Figures 11 and 12, respectively; precipitation of the $Al_5Cu_2Mg_8Si_6$ phase is quite evident. Though the equilibrium isopleth diagram

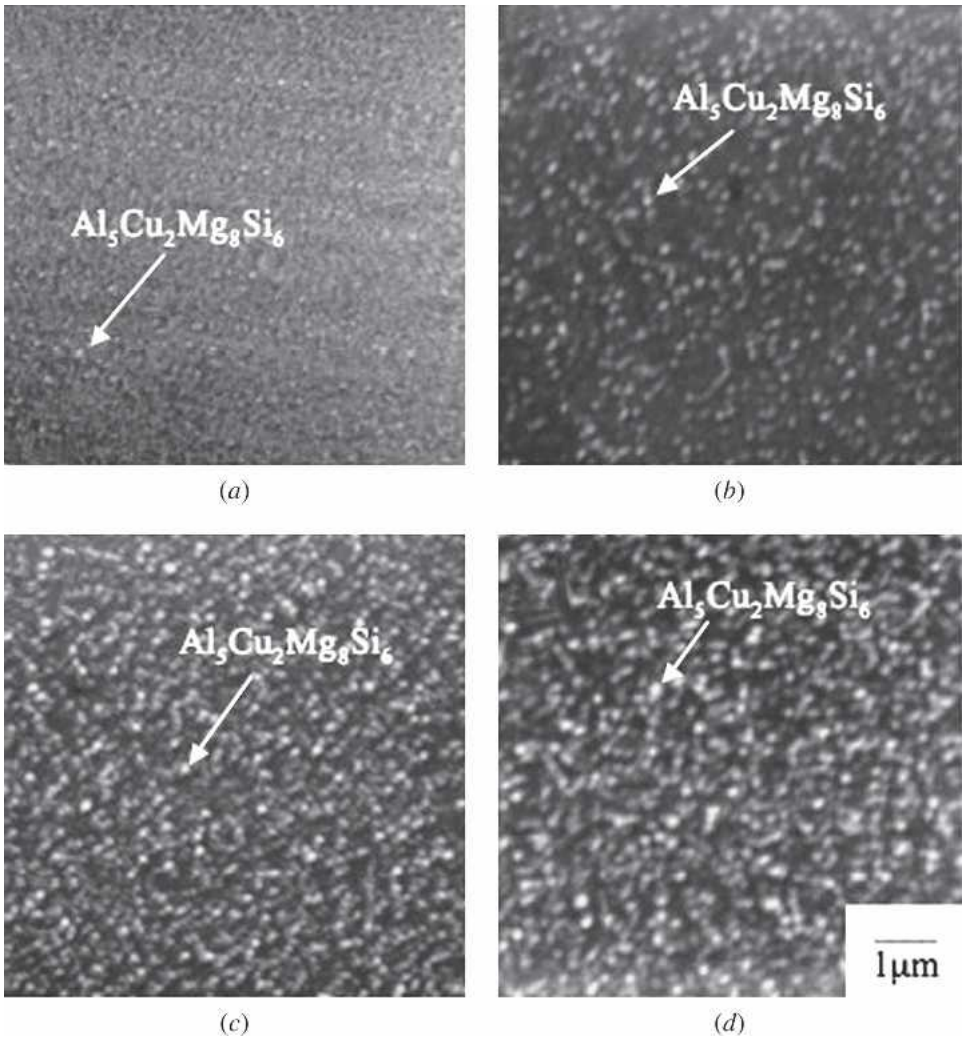

Fig. 12—SEM micrograph of 319 alloy solutionized in the FB at 493 °C for 45 min, quenched in water, and aged using an FB at 240 °C for (*a*) 30 min, (*b*) 60 min, and (*c*) 120 min and (*d*) aged using a CF for 300 min at 240 °C.

predicts the formation of Mg_2Si particles during aging, no Mg_2Si particles were observed. Reasons why these particles were not observed are as follows. (1) The growth/coarsening rate of Mg_2Si particles is low and consequently their particle size may be so small that it is hard to resolve *via* SEM. (2) Since the amount of Cu present in the 319 alloy is greater (2.76 pct) than that in 354 alloy (~1.8 pct), more Mg is tied up with Cu resulting in the formation of $Al_5Cu_2Mg_8Si_6$ phase and thus dominating the nucleation event.

Microstructural observations indicate that the nucleation rate of $Al_5Cu_2Mg_8Si_6$ particles is greater in the alloy aged at 200 °C, as compared to those aged at 240 °C. The number density of $Al_5Cu_2Mg_8Si_6$ particles increases up to 120 minutes of aging in the FB, beyond which a decrease in the number density is noted. This infers that nucleation of $Al_5Cu_2Mg_8Si_6$ particles is completed in less than 2 hours of aging in the FB, beyond which coarsening takes place. Coarsening of $Al_5Cu_2Mg_8Si_6$ particles takes place through coalescence of smaller particles, which also explains the reason for the decrease in the number of $Al_5Cu_2Mg_8Si_6$ particles in samples aged for times longer than 120 minutes.

C. *Thermal Analysis*

Figure 13 shows the thermal analysis of 319 alloy during solution heat treatment using the FB and CF. An exothermic reaction occurs during solution heat treatment, which is due to the recrystallization and coarsening of the eutectic grains. When solutionizing takes place in the CF, the start and end temperatures of the exothermic reaction are 240 °C and 315 °C, respectively; whereas for the FB-processed alloy, these temperatures are 180 °C and 230 °C, respectively. From Figure 13, it is clearly evident that the exothermic reaction takes place at a lower temperature in the FB than in the CF. This is due to the high heating rate in the FB. A similar observation has been made on the effect of heating rate on recrystallization.[27] The high heating rate generates high thermal stresses and consequently lowers the onset temperature of transformation(s). The same trend was also observed in 354 alloy.

Thermal analysis of 319 alloy during aging is shown in Figure 14. Prior to aging, the alloy was solutionized for 45 minutes at 493 °C using the FB and naturally aged for 48 hours. Two endothermic transformations are observed during aging in the CF. The first transformation starts at

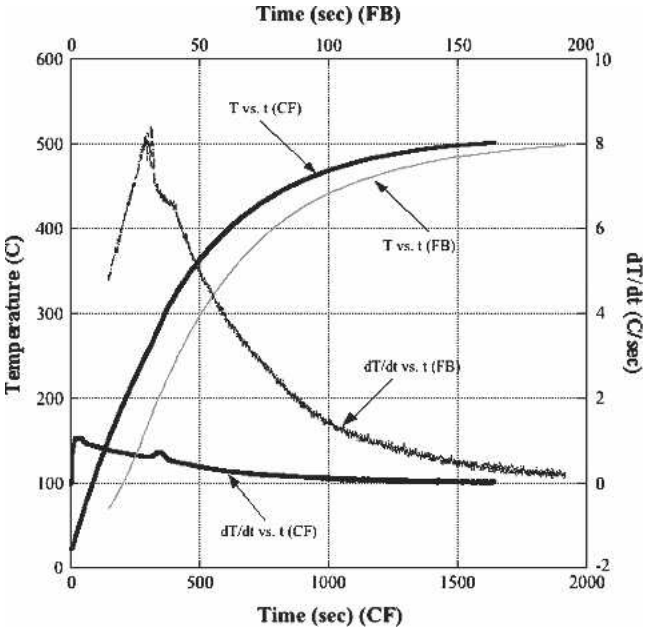

Fig. 13—Thermal analysis of 319 type alloy during solution heat treatment using a CF and an FB.

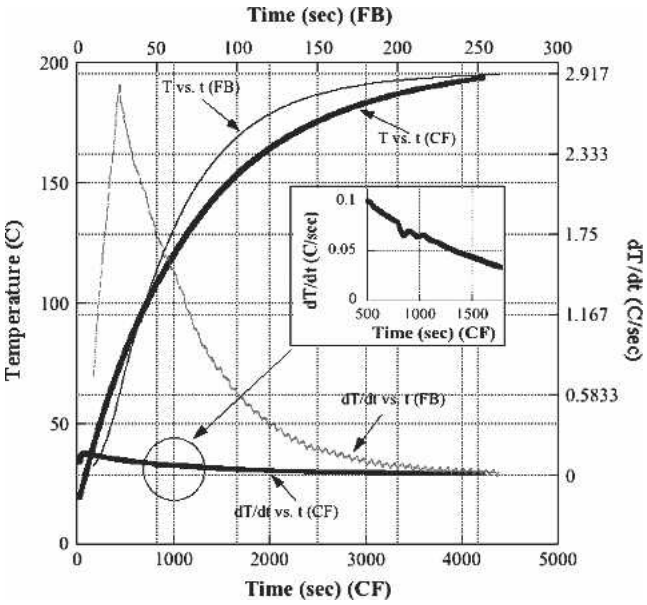

Fig. 14—Thermal analysis of 319 type alloy during aging using a CF and an FB.

106 °C and ends at 112 °C, while the second transformation starts at 112 °C and ends at 119 °C. In contrast, no endothermic reaction is observed during aging in the FB. It may be noted that precipitation is an exothermic reaction. This shows that prior to precipitation, two endothermic transformations take place. The first one may be due to the dissolution of GP zones and the second one may be due to the dissolution of metastable cluster(s)/co-cluster of combinations of Cu, Mg, and Si. These GP zones are formed during natural aging. Similar observations were made by Li *et al.*,[9] who observed the dissolution of GP

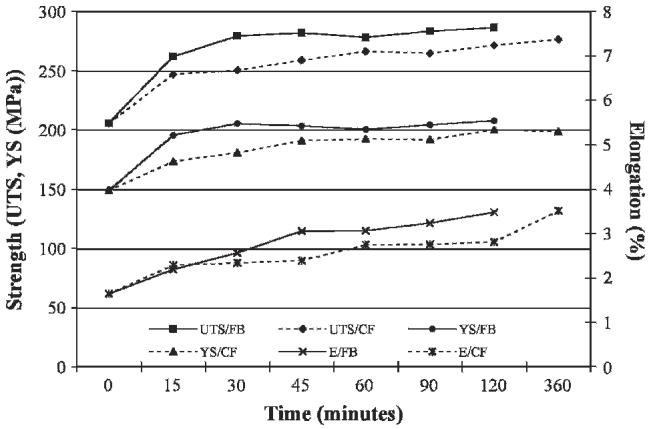

Fig. 15—Variation in UTS, YS, and elongation (E) of 354 alloy solutionized at 527 °C.

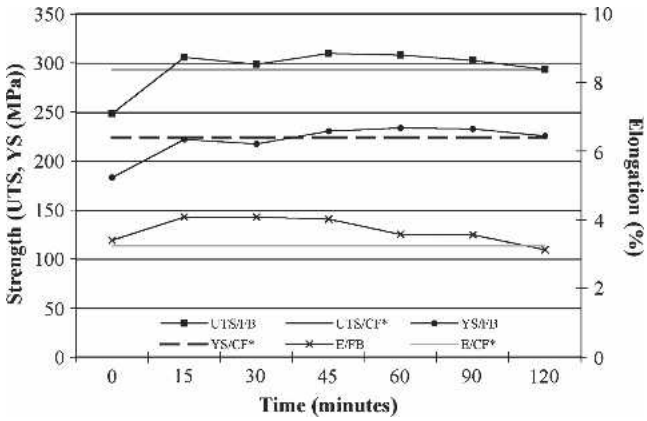

Fig. 16—The effect of solution heat-treatment time (T4 condition) on UTS, YS, and elongation (E) of 319 alloy using a FB reactor. Note: 0 time refers to the as-cast condition and the straight lines (without marker data points) are for the alloy solution heat treated at 493 °C for 6 h in a CF.

zones in cast Al-Si-Cu-Mg alloy (containing 1.48 wt pct of Mg) during the initial stage of aging. This endothermic reaction plays a vital role and decreases the precipitation rate during aging. Similar thermal analyses results were found for 354 alloy. Further work with TEM and local electrode atom probe (LEAP) microscope is being carried out to confirm the mechanisms giving rise to these observed effects of heating rate on the nucleation of precipitates.

D. *Tensile Properties*

1. *Effect of T4 temper (solution heat treatment and quenching)*

a. *354 alloy*

The effect of solution heat treatment on tensile properties of 354 alloy is shown in Figure 15. In general, solution heat treatment of alloys using the FB shows marginally improved tensile properties than the conventionally treated alloy. As expected, the UTS increases with solutionizing time for both the FB- and CF-treated alloys. In the former (FB), the optimum value of UTS is attained within 30 minutes, while in the latter (CF), it takes about 60 to 90 minutes. The effect of solutionizing on elongation is

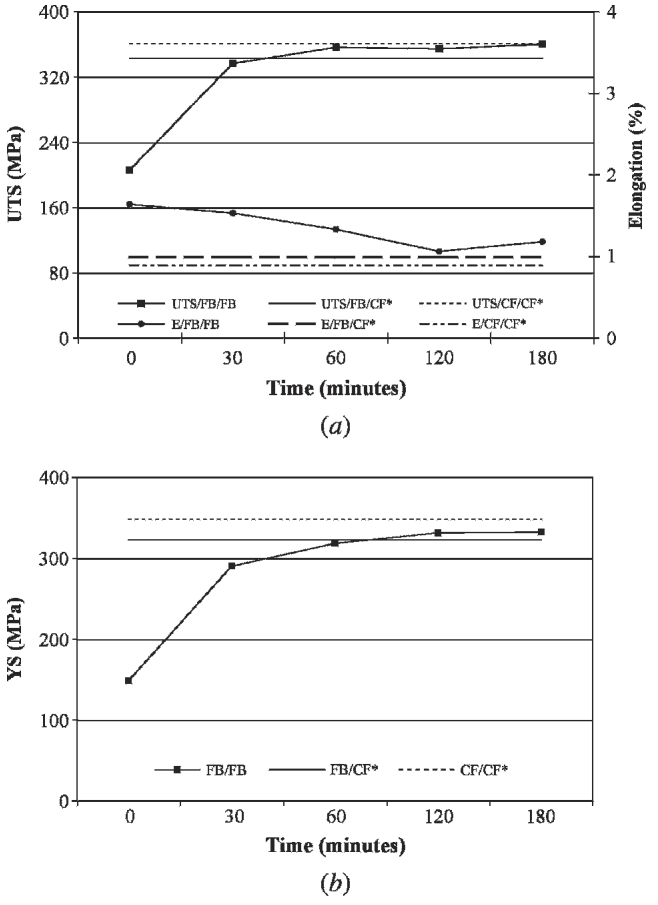

Fig. 17—Effect of aging 354 alloy at 200 °C on (*a*) UTS and elongation (E) and (*b*) YS. Note: FB/FB: FB solutionized and FB aged; FB/CF*: FB solutionized and CF aged; and CF/CF*: CF solutionized and CF aged. Aging time for FB/CF* and CF/CF* is 5 hours.

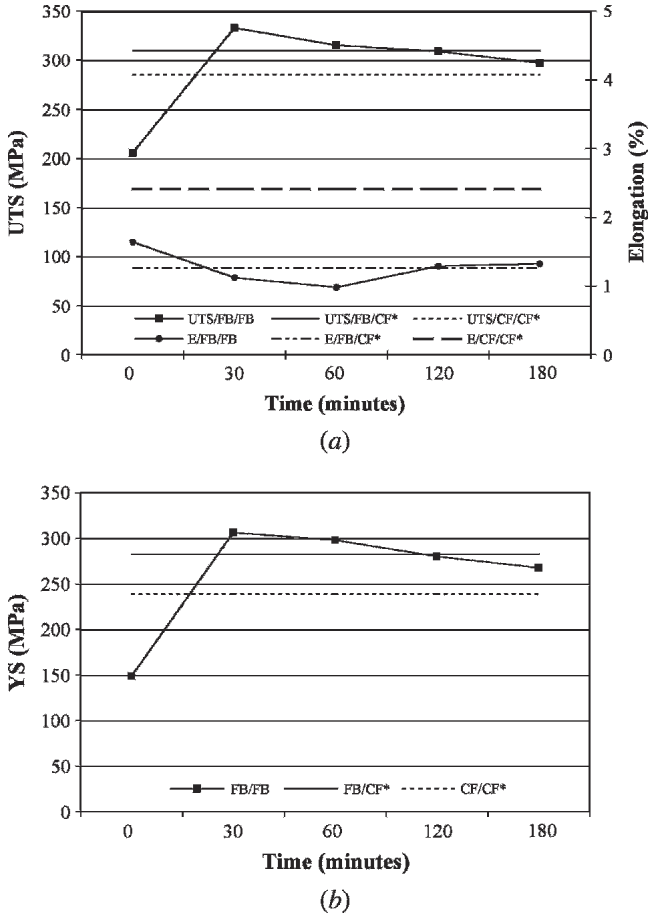

Fig. 18—Effect of aging 354 alloy at 240 °C on (*a*) UTS and elongation (E) and (*b*) YS. Note: FB/FB: FB solutionized and FB aged; FB/CF*: FB solutionized and CF aged; and CF/CF*: CF solutionized and CF aged. Aging time for FB/CF* and CF/CF* is 5 hours.

shown in Figure 15. Elongation increases significantly within 60 minutes in the FB-processed alloy, beyond which no significant change is observed. An increase in YS (Figure 15) is observed in both FB and conventionally solutionized samples. The increase in YS on solution heat treatment is due to the combined effect of solid solution strengthening and the formation of GP zones or co-clusters (in the size range of <5 nm) during natural aging.

b. *319 alloy*

The effect of solution heat treatment on UTS, YS, and elongation of Sr-modified 319 alloy is shown in the Figure 16. As expected, the UTS value increases with solution heat-treatment time using FB. However, a small decrease in UTS is observed beyond 30 minutes; this is due to the effect of matrix hardening and thereby reduction in the ductility of the alloy. Solution heat treatment increases YS. No significant effect on ductility is observed after solution heat treatment in both the FB and CF.

2. *Effect of T6 temper (solution heat treatment, quenching, and aging)*

a. *354 alloy*

Effects of the FB aging at 200 °C and 240 °C on UTS, elongation, and YS are shown in Figures 17(a) and (b) and 18(a) and (b), respectively. Reasonably high strength and good ductility are achieved using the FB within 60 minutes. The strength and ductility (*i.e.,* elongation) of samples aged for 60 minutes in the FB are close to those aged using a CF for 5 hours. From Figures 17 and 18, it is clear that on aging both UTS and YS increase with increasing aging times. On aging at 200 °C, both UTS (Figure 17(a)) and YS (Figure 17(b)) increase significantly within the first 60 minutes. The as-cast UTS and YS are 205.5 and 148.7 MPa, respectively, whereas on aging for 60 minutes at 200 °C in the FB, the UTS and YS are 356.3 and 318.2 MPa, respectively. Beyond 60 minutes of aging in the FB, the increase in both the UTS and YS are marginal. Moreover, the UTS and YS values of the alloy aged in the CF for 300 minutes are close to the value for the alloy aged in the FB for 60 minutes.

Two distinct solutionizing methods were followed prior to aging in the CF for 5 hours. In one case, the alloy was solutionized using the FB for 45 minutes; and in the second case, the alloy was solutionized using a CF for 360 minutes. Both UTS and elongation of the CF-solutionized alloy were marginally greater than the FB-solutionized alloy. This is because longer solution heat-treatment time (360 minutes) in the CF-solutionized alloy results in greater dissolution of the Al_2Cu phase, which consequently results in a greater

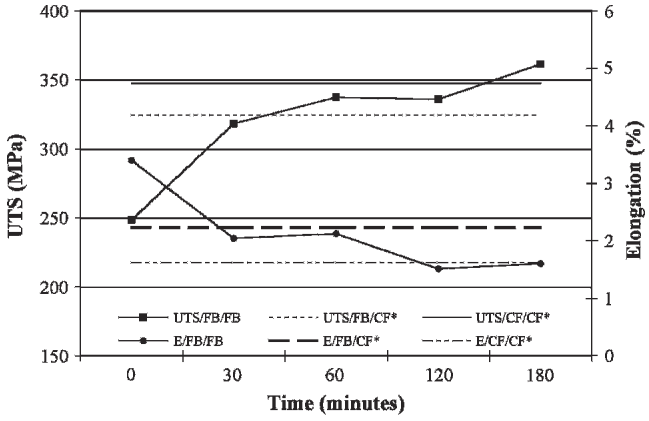

(*a*)

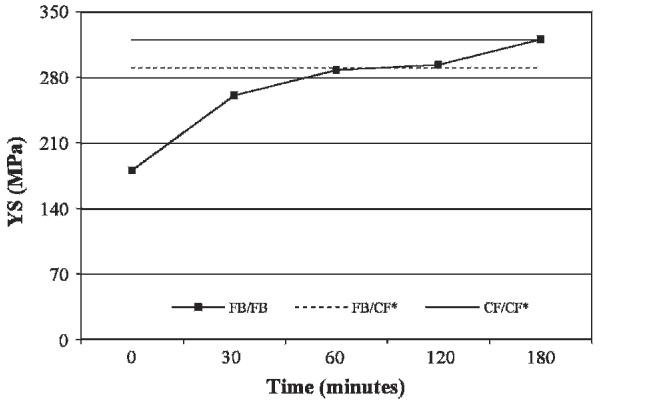

(*b*)

Fig. 19—Effect of aging 319 alloy at 200 °C on (*a*) UTS and elongation (E) and (*b*) YS. Note: FB/FB: FB solutionized and FB aged; FB/CF*: FB solutionized and CF aged; and CF/CF*: CF solutionized and CF aged. Aging time for FB/CF* and CF/CF* is 5 h.

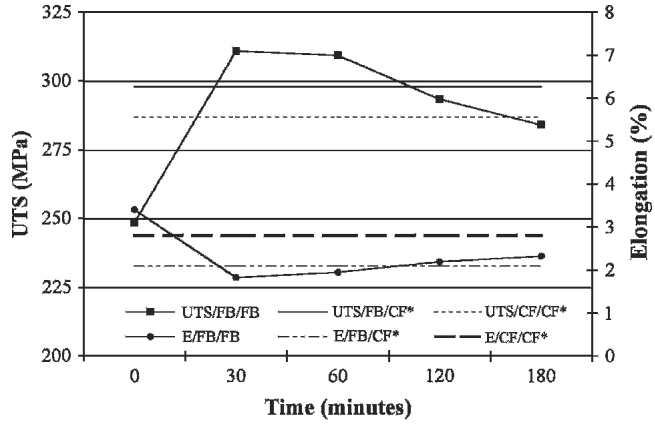

(*a*)

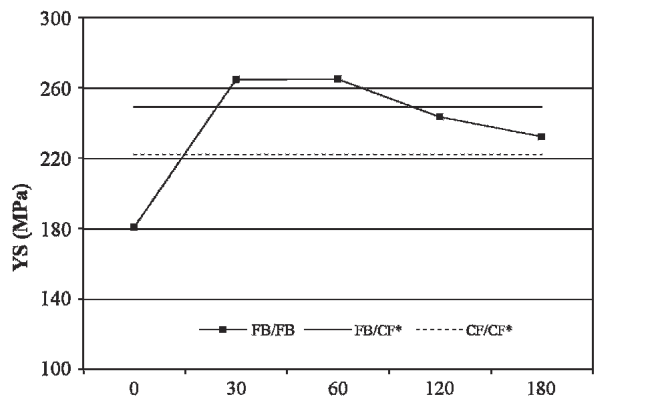

(*b*)

Fig. 20—Effect of aging 319 alloy at 240 °C on (*a*) UTS and elongation (E) and (*b*) YS. Note: FB/FB: FB solutionized and FB aged; FB/CF*: FB solutionized and CF aged; and CF/CF*: CF solutionized and CF aged. Aging time for FB/CF* and CF/CF* is 5 h.

number of precipitates during subsequent aging. However, as compared to the FB-solutionized, CF-aged (for 300 minutes) alloy, the FB-solutionized, FB-aged alloy (for 60 minutes) shows greater UTS and YS values. This is due to the greater precipitation rate in the FB-aged alloy *vis-à-vis* CF-aged alloy. In contrast, the elongation decreases monotonically from 1.64 in the as-cast condition to 1.06 after 120 minutes of aging in the FB. Beyond 120 minutes of aging, there is a marginal increase in the elongation; the increase in elongation after 180 minutes of aging could be due to statistical variations. The elongation of the alloy after 60 minutes of aging in the FB is greater than those aged using CF for 300 minutes at 200 °C.

Aging at 240 °C in the FB shows that both UTS and YS values increase for the first 30 minutes *vis-à-vis* the as-cast alloy. The UTS and YS after 30 minutes at 240 °C in the FB are 309.5 and 306.1 MPa, respectively. Beyond 30 minutes of aging in the FB at 240 °C, both UTS and YS values of the alloy decrease marginally. In general, UTS and YS values for the alloy aged at 240 °C are lower than those aged at 200 °C; this is due to a lower number of precipitates at 240 °C compared to 200 °C. Elongation values of the alloy aged at 240 °C (1.1 to 1.3 pct) for various times are similar to those aged at 200 °C (1.1 to 1.5 pct) and are lower than the as-cast elongation (1.64 pct).

Table IV. Volume Fraction of Precipitating Phases in 354 and 319 Alloys Predicted by the Equilibrium Phase Diagram

	354 Alloy		319 Alloy	
Precipitating Phase	Weight Fraction at 200 °C	Weight Fraction at 240 °C	Weight Fraction at 200 °C	Weight Fraction at 240 °C
$Al_5Cu_2Mg_8Si_6$	1.44	1.09	0.96	0.94
Al_2Cu	2.65	2.62	4.59	4.44

b. *319 alloy*

Effects of aging on UTS, elongation, and YS of 319 alloy at 200 °C and 240 °C are shown in Figures 19(a) and (b) and 20(a) and (b), respectively. Both UTS and YS increase monotonically with aging times at 200 °C in the FB-aged alloy. The UTS and YS values in the as-cast condition are 248.4 and 180.6 MPa, respectively; whereas those aged in FB for 60 minutes are 318.2 and 287.7 MPa, respectively. In general, both UTS and YS increase significantly within the first 60 minutes of aging, beyond which the increase is marginal. Contrary to the increasing trends in UTS and YS values, elongation decreases monotonically with aging time.

Aging at 240 °C results in greater UTS and YS values as compared to the as-cast alloy. With increasing time, both UTS and YS increase significantly within 30 minutes, beyond which both UTS and YS decrease with time. In general, values of both UTS and YS for the alloy aged at 240 °C in the FB are lower than those aged at 200 °C. Elongation values of the alloy aged at 240 °C are in the range of 1.82 to 2.32 pct (depending upon the aging time) and are lower than the as-cast condition.

For both 354 and 319 alloys, the reason for the lower strength of aged samples at 240 °C as compared to those at 200 °C can be explained through isopleths. The predicted fraction of precipitating phases at 200 °C and 240 °C is given in Table IV. It is clear that for both 354 and 319 alloys, the amount of precipitating phases at 200 °C is greater than at 240 °C; the strength of the aged alloy increases with increasing volume fraction of precipitating phase(s).[28] This is consistent with microstructural observations (Section III–B).

IV. CONCLUSIONS

1. Fluidized bed technology provides an efficient heat treating method as compared to CF; heating rates in FB are higher than CF. Significant spherodization of eutectic Si in 354 and 319 alloys is achieved within 30 minutes of solution heat treatment in FB, beyond which the change is marginal, whereas it took 60 minutes to obtain a similar order of sphericity of eutectic Si in CF.
2. The $Al_5Cu_2Mg_8Si_6$ phase dissolved completely within 45 minutes in both 354 and 319 alloys during solution heat treatment in FB. The Mg_2Si phase dissolves completely within 45 minutes of FB solution heat treatment in the Al matrix of the 319 alloy. The dissolution rate of solutes ($Al_5Cu_2Mg_8Si_6$ or Mg_2Si) is greater during FB treatment as compared to CF. This is attributed to the morphological changes during the heating stage. A slower heating rate decreases the matrix/particle interfacial area due to the coarsening of the agglomerates.
3. The short solution heat treatment using FB (2 hours) does not lead to any significant morphological changes of Al_2Cu particles (319 alloy). This is attributed to the blocky morphology of Al_2Cu particles, which has a low matrix/particle interface energy. Similarly, no significant change of the morphology of Fe-rich intermetallics within 120 minutes of solution heat treatment in FB is observed. On prolonged solution heat treatment for 360 minutes in CF, a reduction in angularity of Fe-rich phase is observed. However, the reduction of angularity does not play any significant role in tensile properties.
4. The optimum solution heat-treatment time for 354 and 319 alloys is 45 minutes using FB, beyond which no significant change in tensile properties (UTS, YS, and elongation) is observed.
5. $Al_5Cu_2Mg_8Si_6$ particles precipitate during aging in the matrix of 354 and 319 alloys. These particles are the primary strengthening agents in Al-Si-Cu-Mg alloys. In general, the precipitation rate of $Al_5Cu_2Mg_8Si_6$ particles is greater in FB *vis-à-vis* CF. This effect is attributed to the dissolution of GP zones/clusters of Cu-Mg-Si during the heat-up stage prior to isothermal holding (aging) using CF. This is evident from the thermal analysis results indicating two endothermic transformations (CF aging). In contrast, no endothermic transformation is observed during aging using FB. The high heating rate in FB does not allow sufficient time for the dissolution of the GP zones. These GP zones are well-known heterogeneous sites for nucleation.
6. The coalescence of smaller particles is the dominant mechanism for coarsening of $Al_5Cu_2Mg_8Si_6$ particles in both 354 and 319 alloys.
7. Aging of both 354 and 319 alloys at 200 °C results in greater strength (UTS and YS) as compared to those aged at 240 °C. This is because the weight fraction of precipitates and the number density of precipitates in both alloys (319 and 354) aged at 200 °C are greater than those aged at 240 °C.
8. FB technology is an energy efficient technology for heat treating Al castings. Using FB, the aging time can be reduced to about an hour as compared to 5 hours of aging time in CF. Total heat-treatment time for the T6 temper is less than 2 hours using FB.

ACKNOWLEDGMENTS

The authors are thankful to Montupet (Nogent Sur Oise, France) and Amcast Industrial Corp. for supplying 319 and 354 alloys, respectively. The authors also thank the consortium members of the Advanced Casting Research Center, Metal Processing Institute, WPI, for their support of this work.

REFERENCES

1. D. Apelian, S. Shivkumar, and G. Sigworth: *AFS Trans.*, 1989, vol. 89–137, pp. 727-41.
2. *ASM Handbook*, vol. 2, *Properties and Selection: Nonferrous Alloys and Special-Purpose Materials*, ASM INTERNATIONAL, Materials Park, OH, 1991, pp. 159-67.
3. S. Shivkumar, L. Wang, and C. Keller: *Z. Metallkd.*, 1994, vol. 85 (6), pp. 394-99.
4. Z. Li, A.M. Samuel, F.H. Samuel, C. Ravindran, S. Valtierra, and H.W. Doty: *Mater. Sci. Eng., A*, 2004, vol. 367 (1–2), pp. 96-110.
5. A.M. Samuel and F.H. Samuel: *Metall. Mater. Trans. A*, 1995, vol. 26A (9), pp. 2359-72.
6. E.J. Martinez, M.A. Cisneros, S. Valtierra, and J. Lacaze: *Scripta Mater.*, 2005, vol. 52 (6), pp. 439-43.
7. L. Backerud, G. Chai, and J. Tamminen: *AFS/SKANALUMINIUM*, 1990, vol. 71, pp. 79-85.
8. J.H. Sokolowski, M.B. Djurdjevic, C.A. Kierkus, and D.O. Northwood: *J. Mater. Processing Technol.*, 2001, vol. 109 (1–2), pp. 174-80.
9. R.X. Li, R.D. Li, Y.H. Zhao, L.Z. He, C.X. Li, H.R. Guan, and Z.Q. Hu: *Mater. Lett.*, 2004, vol. 58 (15), pp. 2096-101.
10. D.L. Zhang and L. Zheng: *Metall. Mater. Trans. A*, 1996, vol. 27A (12), pp. 3983-991.
11. S. Zafar, N. Ikram, M.A. Shaik, and K.A. Shoaib: *J. Mater. Sci.*, 1990, vol. 25 (5), pp. 2595-97.
12. H.G. Kang, M. Kida, H. Miyahara, and K. Ogi: *AFS Trans.*, 1999, vol. 107, pp. 507-15.
13. P. Oullet and F.H. Samuel: *J. Mater. Sci.*, 1999, vol. 34 (19), pp. 4671-97.
14. H. Beumler, A. Hammerstad, B. Wieting, and R. Dasgupta: *AFS Trans.*, 1986, vol. 96, pp. 1-12.
15. S.K. Chaudhury, L. Wang, and D. Apelian, *AFS Trans.*, 2004, vol. 112, Paper 04-055, pp. 1-16.

16. R.W. Reynoldson: *Heat Treatment in Fluidized Bed Furnaces*, ASM INTERNATIONAL, Materials Park, OH, 1995, pp. 34-36.
17. J. Keist: *J. Met.*, 2005, vol. 57 (4), pp. 34-39.
18. D. Apelian and S.K. Chaudhury: *J. Phys. IV*, 2004, vol. 120, pp. 555-62.
19. D. Holland-Moritz, D.M. Herlach, and K. Urban: *Physical Rev. Lett.,* 1993, vol. 71 (8), pp. 1196-99.
20. X. Yan, L. Ding, S.L. Chen, F. Xie, M. Chu, and Y.A. Chang: *Light Metals*, 130th TMS Annual Meeting, New Orleans, LA, Feb. 11-15, 2001, TMS, Warrendale, PA, 2001, pp. 1091-97.
21. S.L. Chen, F. Zhang, S. Daniel, F.Y. Xie, X.Y. Yan, Y.A. Chang, R. Schmid-Fetzer, and W.A. Oates: *J. Met.*, 2003, vol. 55 (12), pp. 48-51.
22. M.H. Mulazimoglu, N. Tenekdijev, B.M. Closet, and J.E. Gruzleski: *Cast Met.*, 1993, vol. 6, pp. 16-28.
23. L.A. Narayanan, F.H. Samuel, and J.E. Gruzleski: *Metall. Mater. Trans. A*, 1994, vol. 25A (8), pp. 1761-73.
24. Q.G. Wang and C.J. Davidson: *J. Mater. Sci.*, 2001, vol. 36 (3), pp. 739-50.
25. M. Caudillo, M. Herrera-Trejo, M.R. Castro, E. Ramirez, C.R. Gonzalez, and J.I. Juarez: *J. Biomed. Mater. Res. A*, 2002, vol. 59 (2), pp. 378-85.
26. F. Vermolen, K. Vuik, and S. Van der Zwaag: *Mater. Sci. Eng. A*, 1998, vol. 254 (1–2), pp. 13-32.
27. M. Slamova, M. Karlik, M. Cieslar, B. Chalupa, and P. Merle: *Kovove Mater.*, 2002, vol. 40 (6), pp. 389-401.
28. C.H. Caceres, J.H. Sokolowski, and P. Gallo: *Mater. Sci. Eng. A*, 1999, vol. 271 (1–2), pp. 53-61.